eV), which was used as an internal standard. Resolution was maintained between 20 and 50 meV for the argon line. All ionization energies were read as the band maxima unless noted otherwise and are the average of at least three different runs. Ionization energy data are accurate to ca. ±0.02 eV.

Acknowledgment. The authors are grateful to the National Science Foundation and the Robert A. Welch Foundation for generous financial support. We also thank Mr. D. E. Schiff for experimental assistance.

Registry No. **1**, 14418-26-9; **1a**, 15199-21-0; **1b**, 15199-22-1; **1c**, 68378-99-4; **1d**, 15199-24-3; **2a**, 71771-37-4; **2b**, 71771-38-5; **2c**, 71771-39-6; **3**, 100-97-0; **5**, 53597-69-6; **5a**, 53597-70-9; **5b**, 56796-56-6; **5c**, 79568-42-6; **6**, 56971-16-5; **6a**, 56971-17-6; **7**, 1608-26-0; **7a**, 680-31-9; **7b**, 3732-82-9; **7c**, 7422-73-3; **7d**, 7319-05-3.

Contribution from the Department of Chemistry, Florida Atlantic University, Boca Raton, Florida 33431

Electrochemistry, Spectroelectrochemistry, and Electron Paramagnetic Resonance Spectroscopy of Aqueous Molybdenum(VI), -(V), -(IV), and -(III) Catechol Complexes. Stabilization of Reduced Monomers in Weakly Alkaline Solution

LYNN M. CHARNEY, HARRY O. FINKLEA, and FRANKLIN A. SCHULTZ*

Received January 13, 1981

Stable, monomeric Mo(V), -(IV), and -(III) catechol complexes are generated by electrochemical reduction of the *cis*-dioxomolybdenum(VI) monomer $MoO_2(cat)_2^{2-}$ in pH >9 aqueous buffers containing excess catechol. The four oxidation states are interconverted within a range of ~450 mV. We have characterized the Mo(VI)–Mo(III) oxidation states by bulk solution electrochemistry, EPR spectroscopy, and visible wavelength spectroelectrochemistry in Hg(Au)-minigrid, thin-layer electrode cells. Coordination reactions at aquo sites produced upon reduction of Mo oxo groups stabilize the reduced monomers and influence their subsequent redox chemistry. The Mo(V) monomer is identified as $MoO(Hcat)(cat)_2^{2-}$, which bears a monodentate, monoprotonated catechol ligand cis to the Mo=O group. This monomer exists in equilibrium with 10–20% di-μ-oxo molybdenum(V) dimer at pH >9 and 1–2 mM Mo. The Mo(IV) and -(III) complexes are formulated as tris(catecholato) complexes which constitute a reversible $Mo(cat)_3^{2-/3-}$ redox pair. The former species may in fact contain coordinated semiquinone as $Mo^{III}(SQ)(cat)_2^{2-}$. This material is formed by two-electron reduction of $MoO(Hcat)(cat)_2^{2-}$ to $Mo(H_2O)(Hcat)(cat)_2^{2-}$, closure of the third catechol chelate ring in the Mo(III) electrode product, and *oxidative* transfer of one electron. At more positive potentials, $Mo(cat)_3^{2-}$ is oxidized irreversibly to the Mo(V) and -(VI) oxo species. Aqueous molybdenum–catechol electrochemistry therefore consists of structurally distinct Mo(VI)/Mo(V), Mo(V)/Mo(III), and Mo(IV)/Mo(III) redox couples cyclically linked by irreversible coordination and redox reactions.

In a previous paper[1] we described the electrochemistry of the *cis*-dioxo molybdenum(VI)–catechol complex, $MoO_2(cat)_2^{2-}$, in pH 3.5–7 aqueous buffers. Under these conditions, $MoO_2(cat)_2^{2-}$ is reversibly reduced to Mo(V) and Mo(III) monomers, but these species are only transiently stable. The principal means of deactivation after reduction to the Mo(V) state is dimerization, which proceeds through aquo or hydroxo sites on the metal. Partial coordination of pyridine at an aquo site on Mo(V) slows the rate but does not block the ultimate process of dimer formation.

Production of reduced molybdenum monomers in aqueous media is of interest in the bioinorganic and coordination chemistry of this element.[2] We therefore sought conditions which would stabilize monomeric electrode products by investigating the electrochemistry of $MoO_2(cat)_2^{2-}$ in more alkaline (pH 7–10) solutions. At pH ≥9 stable Mo(V), -(IV), and -(III) monomers can be generated electrochemically from $MoO_2(cat)_2^{2-}$. The present paper describes our efforts in characterizing these species and the processes by which they are formed using techniques of cyclic voltammetry, controlled-potential coulometry, EPR spectroscopy, and visible-wavelength spectroelectrochemistry[3] at optically transparent thin-layer electrodes.

Experimental Section

For spectroelectrochemical experiments, an optically transparent thin-layer electrode (OTTLE) cell with an amalgamated gold (Hg–Au) minigrid working electrode was constructed from a Teflon block following the design of Anderson et al.[4] A quartz plate was sealed against a silicone O-ring on the Teflon block by means of a pressure plate and four bolts. Internal Teflon strips served as spacers to control cell thickness. The gold minigrid (2000 lines/in., Buckbee-Mears Co., St. Paul, MN) was contained completely within the volume defined by the O-ring to avoid possible leakage across an O-ring/minigrid seal. Electrical contact with the grid was made by passing a gold rod through the Teflon block and sealing it in place with a hollow screw and a small O-ring. The entire cell could be readily disassembled for replacement of the gold mesh. The authors will provide details of construction upon request.

The published procedure for amalgamating a gold minigrid was modified. The cell was charged with a solution containing saturated mercuric nitrate, 0.5 M KCl, and 0.1 M HCl. Calomel (Hg_2Cl_2) was first deposited galvanostatically with a constant current of 100 μA and then converted to Hg^0 with use of either potentiostatic reduction at −0.4 V vs. SCE or further galvanostatic reduction at 100 μA. This two-step procedure eliminated excessive bubble formation and occasional breaks in electrical contact around the counter electrode of the OTTLE, which occurred if direct potentiostatic reduction of Hg^{2+} at −0.7 V was attempted. Other details of the amalgamation procedure were as described by Meyer et al.[5]

Visible spectra were recorded at a scan rate of 8 nm s^{-1} with the OTTLE cell in a rapid-scan spectrometer (RSS-C, Harrick Scientific Corp., Ossining, NY). For greater stability in these visible measurements, the xenon arc source was replaced by a 75-W tungsten–halogen lamp, powered by a 12-V dc supply (Hewlett-Packard 62012E). The RSS was interfaced to a Nova 2 minicomputer, which provided capabilities for acquisition of spectra, base-line subtraction, data smoothing, and data plotting. The optical thickness (ca. 250 μm) and coulometric volume (ca. 30 μL) of the cell were determined

(1) Charney, L. M.; Schultz, F. A. *Inorg. Chem.* **1980**, *19*, 1527.
(2) Stiefel, E. I. *Progr. Inorg. Chem.* **1977**, *22*, 1.
(3) Kuwana, T.; Heineman, W. R. *Acc. Chem. Res.* **1976**, *9*, 241. Heineman, W. R. *Anal. Chem.* **1978**, *50*, 390A.
(4) Anderson, C. W.; Halsall, H. B.; Heineman, W. R. *Anal. Biochem.* **1979**, *93*, 366.
(5) Meyer, M. L.; DeAngelis, T. P.; Heineman, W. R. *Anal. Chem.* **1977**, *49*, 602.

0020-1669/82/1321-0549$01.25/0

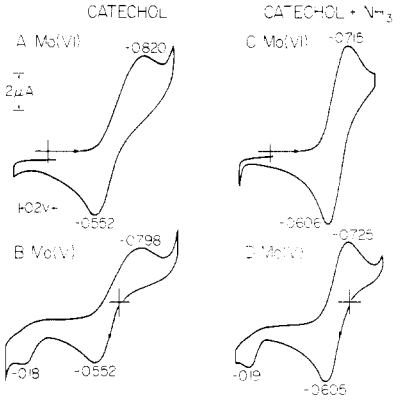

Figure 1. Cyclic voltammograms of $MoO_2(cat)_2^{2-}$ and of Mo(V) solutions produced by its one-electron, controlled-potential reduction: (A and B), 2 mM Mo, 0.15 M H_2cat, 1 M KCl, sweep rate = 50 mV s^{-1}, pH 9.42; (C and D), as in (A) except 1 M NH_4Cl + 1 M NH_3 in place of 1 M KCl and pH 9.85.

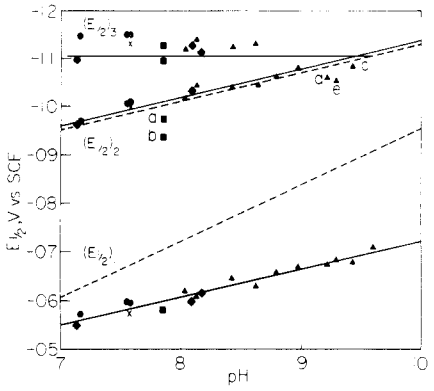

Figure 2. Plots of $E_{1/2}$ vs. pH for Mo(VI)/Mo(V) ($(E_{1/2})_1$), Mo(V)/Mo(III) ($(E_{1/2})_2$), and Mo(IV)/Mo(III) ($(E_{1/2})_3$) redox couples at pH >7 (solid lines). Broken lines are $E_{1/2}$ relationships extrapolated from pH <7. Solutions contain 1 mM Mo, 0.15 M H_2cat and the following buffer components: phosphate (●), Tris (♦), en (■), NH_3 (▲), and catechol alone (×). T = 25 °C, ionic strength = 0.5. Points a–e correspond to solutions containing 0.01 M en, 0.1 M en, 0.18 M NH_3, 0.25 M NH_3, and 0.5 M NH_3, respectively.

with freshly prepared solutions of potassium ferricyanide prior to the amalgamation step. Wavelength was calibrated with a holmium oxide filter.

Argon-purged sample solutions containing $MoO_2(cat)_2^{2-}$, catechol, and buffer and background electrolyte containing catechol and buffer were prepared as described previously.[1] A 50:1 or greater excess of catechol over Mo(VI) was maintained in all solutions to ensure quantitative formation of the 2:1 complex.[6] Anaerobic transfer of solutions to the OTTLE cell was accomplished by using syringes and liquid chromatographic fittings. Precautions for avoiding atmospheric oxidation were adhered to;[1] discoloration of the molybdenum-free electrolyte made such an event detectable. Care is needed because the air sensitivity of catechol increases in alkaline solutions, particularly those that contain ammonia buffer.

Electrochemical equipment and procedures for cyclic voltammetric and coulometric experiments were described previously.[1] The working electrode in voltammetric experiments was a hanging Hg drop of 0.022-cm^2 area. A fresh drop was used for each trial and was exposed to the solution for 30–60 s before measurement. The OTTLE cell was controlled by a battery-powered potentiostat with *iR* compensation and a triangular wave generator, which provided potential sweep rates as low as 1 mV s^{-1}. Potentials are reported vs. the saturated calomel electrode.

Room-temperature EPR spectra were recorded at 9.52 GHz on a Varian V-4502 spectrometer at the Charles F. Kettering Research Laboratory, Yellow Springs, OH. Samples were prepared by controlled-potential electrolysis at a mercury pool cathode and transferred under argon directly to a capillary EPR cell. Mo(V) signal intensities were determined by double integration and comparison to solutions of $K_3Mo(CN)_8$, which were standardized by absorption spectroscopy at 388 nm.[7] The uncertainty of the quantitative EPR measurements is estimated to be ±20%.

Results

The electrochemistry of $MoO_2(cat)_2^{2-}$ was investigated in pH 7–10 solutions buffered with phosphate, ammonia, ethylenediamine (en), tris(hydroxymethyl)aminomethane (Tris), and catechol, itself. Between pH 7 and 9, $MoO_2(cat)_2^{2-}$ is reduced to a Mo(V) monomer, which is stable on the time scale of cyclic voltammetry but which forms a significant amount of Mo(V) dimer in the longer time required for controlled-potential coulometry. Our results focus on the region pH 9–10 where reduced molybdenum–catechol monomers are stabilized most completely.

Molybdenum(VI)–Molybdenum(V) Couple. Figure 1 shows cyclic voltammograms of the Mo(VI)/Mo(V) couple before and after coulometric reduction of $MoO_2(cat)_2^{2-}$ in pH 9.42 catechol buffer and pH 9.85 catechol–ammonia buffer. Under such conditions the cathodic wave appears as a diffusion-controlled, one-electron reduction to a chemically stable product. Its peak current parameter, $i_p/\nu^{1/2}AC$ (corrected for spherical diffusion),[8] is constant for sweep rates of ν = 0.01–30 V s^{-1}, the reverse-to-forward peak current ratio, i_{pr}/i_{pf}, equals unity, and no Mo(V) dimer can be detected when the reverse sweep is extended to the positive potential limit. Controlled-potential reduction of $MoO_2(cat)_2^{2-}$ at potentials 100–150 mV negative of the cathodic peak consumes 1.01 ± 0.08 faradays/mol of Mo (23 trials in catechol, ammonia, en, and Tris buffers). Voltammograms of reduced solutions (Figure 1B,D) exhibit a major oxidation wave at a potential coinciding with the anodic peak of the original Mo(VI)/Mo(V) couple and a minor wave at ca. −0.2 V, which we assign to irreversible oxidation of the di-μ-oxo molybdenum(V) dimer $Mo_2O_4(cat)_2(H_2O)_2^{2-}$[1] on the basis of its linearly pH-dependent peak potential between pH 5.5 and 9.5 (E_p = +0.360 − 0.057(pH)). By comparing the peak current for Mo^V_2 oxidation with that for oxidation of $Mo_2O_4(cat)_2(H_2O)_2^{2-}$ in pyridine buffer[1] and the peak current for Mo(V) monomer oxidation with that observed initially for $MoO_2(cat)_2^{2-}$ reduction, it is possible to estimate the concentrations of Mo(V) monomer and dimer. In solutions containing 0.15 M catechol and 1, 1.5, and 2 mM molybdenum at pH ≥9, 91%, 87%, and 83%, respectively, of the Mo(V) remains monomeric after controlled-potential electrolysis. Coulometric reoxidation at potentials between the Mo^V and Mo^V_2 oxidation waves requires 1 faraday/mol Mo and quantitatively restores the original voltammogram; the anodic Mo(V) dimer wave is not observed after reoxidation.

In alkaline solution the Mo(VI) → Mo(V) reduction wave exhibits characteristics of slow heterogeneous electron transfer: the cathodic wave broadens, the cathodic-to-anodic peak potential separation (ΔE_p) becomes larger than 60 mV, and the cathodic peak potential shifts in the negative direction with increasing sweep rate. These effects become increasingly severe as pH, catechol concentration, and time of contact between electrode and solution increase.[9,10] However, it is

(6) Kustin, K.; Liu, S. T. *J. Am. Chem. Soc.* **1973**, *95*, 2487.
(7) Martin, J. F.; Spence, J. T. *J. Phys. Chem.* **1970**, *74*, 3589.
(8) Nicholson, R. S.; Shain, I. *Anal. Chem.* **1964**, *36*, 706.
(9) The decrease in electron-transfer rate is attributed to ionization of catechol adsorbed on the electrode surface. Catechol is known to be adsorbed on mercury,[11] and its ionization constant in this form should not be altered much from that in bulk solution (pK_a = 9.23).[12] The onset of slow electron transfer coincides with this expected ionization. The presence of adsorbed catecholate anions would be expected to impede electron transfer by presenting an unfavorable electrostatic barrier to the transfer of electrons from the electrode to dinegative $MoO_2(cat)_2^{2-}$. Use of buffers containing high concentrations of positively charged proton donors (e.g., NH_4^+, enH_2^{2+}, enH^+; see Figures 1 and 5) restores electrochemical reversibility to a considerable extent.

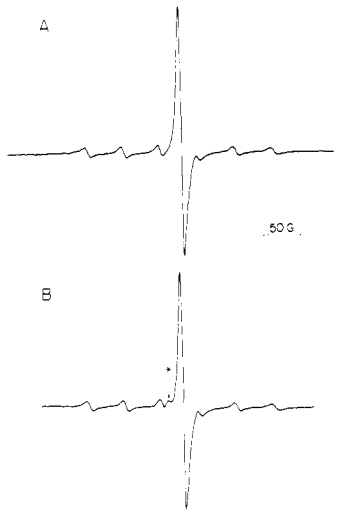

Figure 3. Room-temperature EPR spectra of Mo(V) monomers produced by controlled-potential reduction of $MoO_2(cat)_2^{2-}$ in (A) catechol buffer (0.1 M H_2 cat, 1 M KCl, pH 9.4) and (B) catechol + NH_3 buffer (0.1 M H_2cat, 0.8 M NH_4Cl, 0.8 M NH_3, pH 9.6). Asterisk indicates signal at $g = 1.943$.

possible to determine the half-reaction for $MoO_2(cat)_2^{2-}$ reduction at pH >7 by using an empirical procedure to measure the Mo(VI)/Mo(V) half-wave potential and its changes with solution conditions. Since the anodic wave is less sensitive to the effects of slow electron transfer, $(E_{1/2})_1$ is estimated from cyclic voltammetric sweeps of the Mo(VI)/Mo(V) redox step by extrapolating the *anodic* peak potential (measured at ν = 0.01–0.2 V s^{-1}) to 0 V s^{-1} and subtracting 30 mV.

The solid line in the lower half of Figure 2 is the plot of the Mo(VI)/Mo(V) half-wave potential vs. pH; it follows the relationship $(E_{1/2})_1 = -0.146 - 0.058(pH)$ in V. $(E_{1/2})_1$ is independent of the concentration of ammonia, en, and Tris buffers at constant pH, and also of Mo(VI) concentration. Upon varying catechol concentration (0.02–0.15 M) at constant pH, slopes of $\Delta(E_{1/2})_1/\Delta \log C_{H_2cat} = +58$ mV (pH 9.6 ammonia buffer) and +63 mV (pH 9.4 catechol buffer) are observed.[13] On the basis of these results the Mo(VI)/Mo(V) half-reaction at pH >7 is

$$MoO_2(cat)_2^{2-} + H_2cat + H^+ + e^- \rightleftarrows MoO(Hcat)(cat)_2^{2-} + H_2O \quad (E_{1/2})_1 \quad (1)$$

$Hcat^-$ represents a monoprotonated catechol molecule acting as a monodentate ligand. In acidic buffers the Mo(VI)/Mo(V) half-wave potential in volts follows the relationship[1] $(E_{1/2})_1' = +0.206 - 0.116(pH)$, whose extension is represented by the lower broken line in Figure 2; the half-reaction is

$$MoO_2(cat)_2^{2-} + 2H^+ + e^- \rightleftarrows MoO(H_2O)(cat)_2^- \quad (E_{1/2})_1' \quad (2)$$

(10) Further examples of adsorption-caused retardation of the Mo(VI)/Mo(V) electron-transfer rate occur at Au electrodes in bulk solution and at the Hg(Au) minigrid in the OTTLE cell. Here, too, the severity of the effect increases with increasing time of contact between electrode and solution, presumably because of continuing buildup of adsorbed catechol. Thus, for a Au electrode in pH 8 en buffer, $\Delta E_p = 70$ mV initially but increases to >200 mV within 10 min (ν = 33 mV s^{-1}). Cleaning the electrode restores $\Delta E_p = 70$ mV. In the OTTLE cell the electrode surface cannot be renewed quickly, and because of the longer contact time, $\Delta E_p > 500$ mV (Figure 6).

(11) Ball, N. M. Ph.D. Thesis, University of Wisconsin, Madison, WI, 1969.

(12) Martell, A. E.; Smith, R. M. "Critical Stability Constants"; Plenum Press: New York, 1977; Vol. 3, p 200.

(13) Zelinka et al. reported a similar dependence of $(E_{1/2})_1$ on catechol concentration for the polarographic reduction of $MoO_2(cat)_2^{2-}$ in pH 6.6–7.4 phosphate buffer: Zelinka, J.; Bartusek, M.; Okac, A. *Collect. Czech. Chem. Commun.* **1973**, *38*, 2898.

Table I. Visible Spectra of Molybdenum–Catechol Complexes

Ox state	buffer/pH[a]	λ_{max},[b] nm	ϵ,[b] M^{-1} cm^{-1}
Mo(VI)	all	406	4960
Mo(V)	catechol only/9.3	466 (sh)	2440[c]
	NH_3 (2 M)/9.6	472	2650[c]
	en (1 M)/9.4	471	2680[c]
	Tris (1 M)/10.2	474	2300[c]
Mo(IV)	all	480 (sh)	3700
Mo(III)	all	none detected	

[a] All solutions contain 1 M KCl and 0.15 M catechol in addition to the components listed. [b] Uncertainties in λ_{max} and ϵ are ±5 nm and ±5%. [c] Calculated on the basis of total molybdenum concentration.

When half-reactions 1 and 2 are combined and the bulk concentration and ionization constant ($pK_a = 9.23$)[12] of catechol are taken into account, the equilibrium constant for coordination of $Hcat^-$ to the Mo(V) center is calculated to be $K_f = (1.7 \pm 0.6) \times 10^4$ M^{-1}.

$$MoO(H_2O)(cat)_2^- + Hcat^- \rightleftarrows MoO(Hcat)(cat)_2^{2-} + H_2O \quad K_f \quad (3)$$

EPR Spectroscopy. The room-temperature EPR spectrum of the solution produced by one-electron, controlled-potential reduction of $MoO_2(cat)_2^{2-}$ in pH 9.4 catechol buffer is shown in Figure 3A. On the basis of reaction 1, the signal is assigned to the species $MoO(Hcat)(cat)_2^{2-}$. The parameters $g = 1.933$ and $A(^{95,97}Mo) = 45 \times 10^{-4}$ cm^{-1} (48 G) are consistent with location of the unpaired electron on the molybdenum nucleus. The absorption at $g = 1.933$ is the predominant signal in catechol, tris, en, and ammonia buffers. Its intensity was calibrated against solutions of $K_3Mo(CN)_8$ and compared to the amount of Mo(V) monomer determined from the anodic peak current at ca. –0.6 V in the same solution (see Figure 1B,D). In four experiments using catechol, en, Tris, and ammonia buffers, the concentration of Mo(V) monomer was determined to be 0.91, 0.87, 1.46, and 1.13 mM, respectively, by EPR and 1.01, 1.12, 0.95, and 1.40 mM by voltammetry. Thus, the EPR signal at $g = 1.933$ is quantitatively assigned to the species $MoO(Hcat)(cat)_2^{2-}$ produced in reaction 1. In en and ammonia buffers a second signal, corresponding to ~3% of the total intensity, is observed at $g = 1.943$ (Figure 3B). This signal is attributed to the species $MoO(NH_2R)(cat)_2^-$, produced by a small amount of substitution of amine for $Hcat^-$ in the Mo(V) complex.

Visible Absorption Spectra of Mo(V). Visible absorption spectra of Mo(V) species were obtained by controlled-potential, one-electron reduction of $MoO_2(cat)_2^{2-}$ in the OTTLE cell. Results are uncorrected for the formation of 10–20% Mo(V) dimer, which absorbs only weakly beyond 400 nm. Visible absorption by the Mo(V) monomer in catechol buffer appears as a shoulder at ~466 nm. In ammonia, en, and Tris buffers, the shoulder becomes a clearly defined band which shifts slightly to 470–475 nm. Results are summarized in Table I; spectra of the Mo(V) species are presented later in Figure 7. Although the difference in measured spectral parameters is small, absorption curves in amine buffers are of detectably different shape, and a difference in color is apparent. Reduction of red-orange $MoO_2(cat)_2^{2-}$ in catechol buffer yields a solution with a brownish cast; reduction in amine buffers produces a distinctly redder color. These results agree with the detection by EPR of a small amount of amine-substituted product in en and NH_3 buffers. Since the extent of this substitution is slight, the $MoO(NH_2R)(cat)_2^{2-}$ species must have larger molar absorptivities at ~470 nm than reported in Table I.

Generation of Mo(III) and Mo(IV) Species. Complexities inherent in molybdenum–catechol redox chemistry involving

Table II. Voltammetric Data during Controlled-Potential Reduction and Reoxidation of $MoO_2(cat)_2^{2-}$ in Ammonia Buffer[a]

redox process	Figure	$-E_{pf}$, V	$\lvert E_{pf} - E_{p/2}\rvert$, mV	$-E_{pr}$, V	$i_p/\nu^{1/2}AC$, A cm $s^{1/2}$ mol^{-1} $V^{-1/2}$	i_{pr}/i_{pf}
VI → V	4A	0.828	94	0.658	513	1.04
V → VI	4B	0.640	85	0.821	477	0.96
V → III	4B	1.035 (sh), 1.132[b]			908	
III → IV	4C	1.075	64	1.135	500	1.03
IV → III	4D	1.139	63	1.073	535	0.98
IV → VI	4D	0.626	58		1000	

[a] Conditions: 1 mM Mo(VI), 0.15 M H_2cat, 1.25 M NH_4Cl, 1.25 M NH_3, pH 9.6, sweep rate = 0.05 V s^{-1}. Subscripts f and r refer to forward and reverse sweeps as defined by redox process in first column. [b] Overlapping waves (see text).

these oxidation states are best described by reference to an experiment in which voltammetric traces are recorded at various stages during coulometric reduction and reoxidation of $MoO_2(cat)_2^{2-}$. This is depicted in Figure 4 and Table II for an ammonia-containing buffer; equivalent results are obtained in solutions buffered with catechol alone.

Figure 4A,B shows entire cyclic voltammograms of the system in the Mo(VI) and -(V) states. The results here and in Table II are consistent with the previous characterization of the Mo(VI)/Mo(V) couple as a quasi-reversible one-electron transfer involving a Mo(V) monomer which is stable on the time scale of cyclic voltammetry but which forms a small amount of dimer (visible at the positive extension of the sweep in Figure 4B) on the time scale of controlled-potential coulometry. The first reduction step in the Mo(V) state is approximately twice the height of the Mo(VI) → Mo(V) peak. This observation suggests that the electron-transfer sequence Mo(VI) → Mo(V) → Mo(III), which occurs reversibly, but transiently, at pH <7, also prevails at pH >9. However, a small shoulder is noted on the Mo(V) → Mo(III) wave.

Controlled-potential reduction of Mo(V) or Mo(VI) at −1.40 V proceeds smoothly to a lemon yellow solution and consumes 3 faradays/mol of Mo relative to Mo(VI). A cyclic voltammogram of this solution (Figure 4C) exhibits oxidation waves whose heights correspond to the successive transfer of one and two electrons. If the sweep is reversed after the first anodic peak (broken line, Figure 4C), the cyclic voltammogram has characteristics of a reversible one-electron transfer with a half-wave potential $(E_{1/2})_3 = -1.10$ V.

If the Mo(III) product is reoxidized at −0.87 V, 1 faraday/mol of Mo is required and a cherry red solution is produced. An initial negative scan in this solution (broken line, Figure 4D) and the corresponding data in Table II confirm the existence of a reversible, one-electron couple at −1.10 V. This couple is assigned to reversible electron transfer between Mo(IV) and Mo(III) oxidation states:

$$\text{Mo(IV)} + e^- \rightleftarrows \text{Mo(III)} \quad (E_{1/2})_3 \qquad (4)$$

The same Mo(IV) species is produced by controlled-potential reduction of Mo(VI) at the potential of the second wave (ca. −1.0 V) until 2 faradays/mol of Mo have passed.

Controlled-potential oxidation of the Mo(IV) solution at −0.40 V requires 2 faradays/mol of Mo and quantitatively regenerates the voltammogram of $MoO_2(cat)_2^{2-}$ shown in Figure 4A. Voltammetric oxidation of Mo(IV) (solid line, Figure 4D) is an irreversible process which occurs at a slightly more positive potential than Mo(V) → Mo(VI) oxidation. The Mo(IV) oxidation wave is approximately twice the height and half the width of the Mo(V) oxidation wave (Table II), indicating that two electrons are transferred in this step.

The foregoing results demonstrate that stable molybdenum–catechol complexes in oxidation states Mo(VI)–Mo(III)

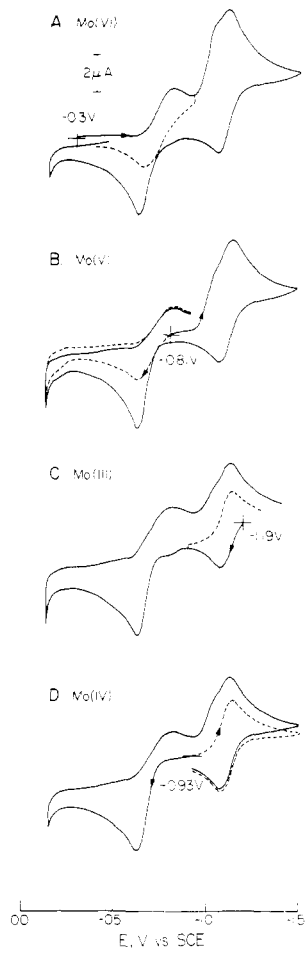

Figure 4. Cyclic voltammograms of molybdenum–catechol complexes in oxidation states VI, V, III, and IV. Broken lines indicate cyclic sweeps restricted to a single redox couple. Conditions as in Table II.

can be generated in aqueous solution above pH 9 and quantitatively interconverted by bulk electrolysis. The pathway is Mo(VI) → Mo(V) → Mo(III) upon reduction and Mo(III) → Mo(IV) → Mo(VI) upon oxidation. This unusual sequence of redox-state conversions also occurs in slow-sweep-rate cyclic voltammetry, as indicated by the relative magnitudes of peak currents in Figure 4. The shapes of the complete cyclic voltammograms are the same in all oxidation states, inferring that the reduced molybdenum species remain monomeric. Full explanation of these observations is presented in the Discussion.

So that there can be a better understanding of the processes leading to formation of the Mo(IV) species, a more extensive cyclic voltammetric study was conducted of the Mo(V) → Mo(III) reduction wave starting with a solution of $MoO_2(cat)_2^{2-}$. The results presented in Figure 5 are for a pH 7.7 en buffer. At the faster sweep rate of 0.2 V s^{-1}, the voltammetry of $MoO_2(cat)_2^{2-}$ appears much as it does at pH <7: a reversible Mo(VI) → Mo(V) reduction followed by a reversible Mo(V) → Mo(III) reduction. However, a small reversible redox couple is detected on the negative side of the Mo(V)/Mo(III) wave. When the sweep rate is decreased to 0.01 V s^{-1}, the Mo(V) reduction wave decreases to a size appropriate to a one-electron transfer and becomes irreversible. Meanwhile, the most negative wave increases in size and develops the appearance of a reversible, one-electron couple. The pH-independent half-wave potential of this wave is −1.11 ± 0.02 V, which is identical with the value of $(E_{1/2})_3$ observed for the Mo(IV)/Mo(III) couple generated by controlled-potential reduction of $MoO_2(cat)_2^{2-}$ at $E < -1.0$ V. We attribute the foregoing behavior to a chemical reaction which transforms

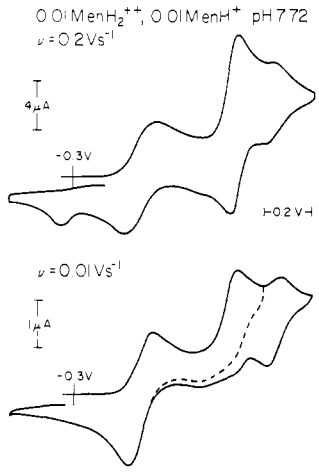

Figure 5. Cyclic voltammetry of $MoO_2(cat)_2^{2-}$ at fast and slow sweep rates in pH 7.7 en buffer. Conditions: 1 mM Mo(VI), 0.15 M H_2cat, ionic strength = 0.5.

the initially reversible Mo(V) ⇄ Mo(III) reduction into an irreversible Mo(V) → Mo(IV) reduction followed by the reversible Mo(IV) ⇄ Mo(III) redox step described in eq 4. This description requires the existence of two chemically distinct Mo(III) species: one reversibly oxidizable to Mo(V) and a second reversibly oxidizable to Mo(IV):

$$\text{Mo(V)} \overset{+2e^-}{\rightleftharpoons} \text{Mo(III)} \rightarrow \text{Mo(III)}' \overset{-e^-}{\rightleftharpoons} \text{Mo(IV)} \quad (5)$$

The behavior represented in Figure 5 is observed in other pH 7–10 buffers. However, the potential of Mo(V) ⇄ Mo(III) reduction shifts in the negative direction and the rate of the chemical reaction increases with increasing pH. Thus, at high pH and slow sweep rates, Mo(V) reduction appears as overlapping one-electron waves with a faintly detectable shoulder as shown in Figure 4A.

Using fast-sweep-rate cyclic voltammetry (ν = 0.1–60 V s^{-1}) it is possible to observe Mo(V) reduction as a reversible two-electron transfer ($i_p/\nu^{1/2}AC \simeq 1000$ A cm $s^{1/2}$ mol^{-1} $V^{-1/2}$) at all but the highest pH values. The reversible half-wave potential obtained from these measurements is plotted as the solid line defined by $(E_{1/2})_2 = -0.557 - 0.058(\text{pH})$ in Figure 2, which suggests the half-reaction

$$MoO(Hcat)(cat)_2^{2-} + 2H^+ + 2e^- \rightleftarrows Mo(H_2O)(Hcat)(cat)_2^{2-} \quad (E_{1/2})_2 \quad (6)$$

for Mo(V) → Mo(III) reduction at pH >7. At pH <7, Mo(V) → Mo(III) reduction occurs by the half-reaction

$$MoO(H_2O)(cat)_2^- + 2H^+ + 2e^- \rightleftarrows Mo(H_2O)_2(cat)_2^- \quad (E_{1/2})_2' \quad (7)$$

whose relationship $(E_{1/2})_2' = -0.547 - 0.58(\text{pH})$ is plotted as a broken line in Figure 2. The similarity of these expressions suggests either that coordination of $Hcat^-$ following Mo(VI) reduction is slow and Mo(V) is therefore reduced as $MoO(H_2O)(cat)_2^-$ at fast sweep rates or that replacement of H_2O by $Hcat^-$ in the Mo(V) coordination sphere does not greatly affect $(E_{1/2})_2$.

In buffers containing en and high concentrations of NH_3, $(E_{1/2})_2$ is shifted positive of the values defined by eq 6 and 7. Representative observations are included in Figure 2. This result is attributed to coordination of amines to the Mo(III) center. Insufficient data were taken for quantitative treatment, but coordination by en appears much stronger than by NH_3, indicating possible formation of chelated species such as $Mo(en)(cat)_2^-$.

Thin-Layer Spectroelectrochemistry. Visible-wavelength thin-layer spectroelectrochemistry was conducted to support the results of bulk solution electrochemistry and as a convenient means of generating and characterizing the oxygen-sensitive electrode products. A cyclic voltammogram of $MoO_2(cat)_2^{2-}$ in pH 9.6 ammonia buffer in the OTTLE cell is shown in Figure 6. The Roman numerals indicate the oxidation state changes associated with each electron-transfer step. The number of electrons transferred in each step was confirmed by controlled-potential coulometry in the thin-layer cell.

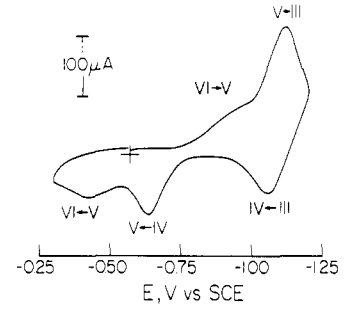

Figure 6. Cyclic voltammogram of $MoO_2(cat)_2^{2-}$ in OTTLE cell: 2 mM Mo(VI), 0.15 M H_2cat, 1 M KCl, 1 M NH_4Cl, 1 M NH_3, pH 9.6, sweep rate = 4 mV s^{-1}.

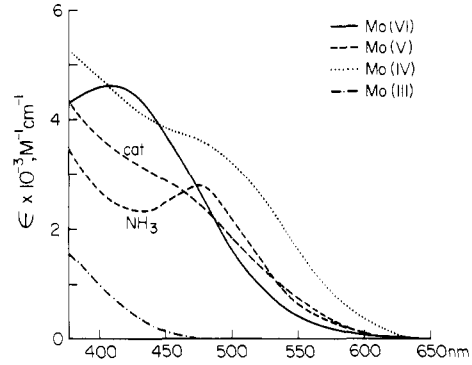

Figure 7. Visible absorption spectra of molybdenum–catechol complexes in various oxidation states recorded in ammonia buffer in OTTLE cell. Conditions as in Figure 6. Conditions are identical for Mo(V) spectrum marked "cat", except NH_4Cl and NH_3 are absent. Potentials applied to generate oxidation states starting with Mo(VI) were as follows: Mo(VI), –0.3 V; Mo(V), –0.88 V (NH_3), –0.95 V (cat); Mo(IV), –1.2 V and then –0.9 V; Mo(III), –1.2 V.

Thin-layer electrochemical results are in agreement with bulk solution experiments with one exception. Slow electron transfer of the Mo(VI)/Mo(V) couple is further retarded in the OTTLE cell[10] so that Mo(VI) reduction is observed at –0.95 V and Mo(V) oxidation at –0.42 V. As a result, Mo(IV) → Mo(V) oxidation (–0.64 V) and Mo(V) → Mo(VI) oxidation (–0.42 V) appear as separate one-electron processes in the thin-layer cell, whereas Mo(IV) → Mo(VI) oxidation occurs in a single step (–0.63 V) in bulk solution (Table II, Figure 4). Other aspects of $MoO_2(cat)_2^{2-}$ thin-layer electrochemistry parallel those in bulk solution: a composite two-electron reduction at –1.12 V and a one-electron oxidation at –1.06 V.

The cyclic voltammogram in Figure 6 illustrates that molybdenum–catechol complexes in oxidation states III–VI can be interconverted by appropriate control of potential in the thin-layer cell. Visible absorption spectra of these species recorded in pH 9.6 ammonia and catechol buffers are shown in Figure 7; spectral data are collected in Table I. The spectrum of each species can be reproduced after cycling through the other oxidation states. Only the spectrum of the Mo(V) product is sensitive to buffer composition. The intensification and small shift in the absorption band at ~470 nm on going from catechol to an amine-containing buffer were

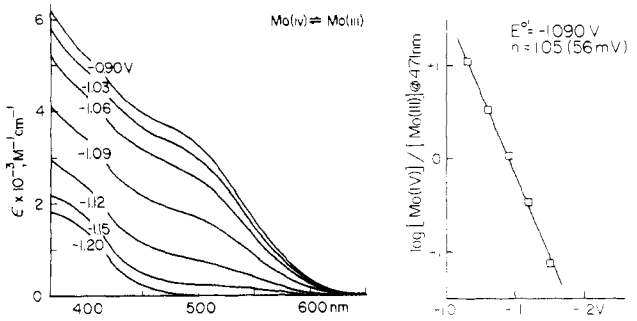

Figure 8. Spectroscopic monitoring and spectropotentiostatic Nernst plot of Mo(IV)/Mo(III) couple. Conditions as in Figure 6.

described previously and are illustrated in Figure 7 for an NH_3 buffer.

Thin-layer spectroelectrochemistry also can provide independent measurement of the formal potential ($E^{\circ\prime}$) and n value of a reversible light-absorbing redox couple. Changes in absorbance are monitored at fixed wavelength as electrode potential is adjusted to values in the range of $E^{\circ\prime}$, allowing time for equilibrium to be achieved within the cell following each change of potential. Results are plotted according to the spectropotentiostatic Nernst equation[14]

$$E = E^{\circ\prime} + \frac{2.3RT}{nF} \log \frac{[O]}{[R]} \qquad (8)$$

The ratio of oxidized to reduced form at each potential is determined from the relationship $[O]/[R] = (A_2 - A_1)/(A_3 - A_2)$, where A_3 is the absorbance of the completely oxidized form, A_1 is the absorbance of the completely reduced form, and A_2 is the absorbance measured for a mixture of O and R.

Room-temperature (22 ± 1 °C) results for the Mo(IV)/Mo(III) couple in pH 9.6 ammonia buffer with spectral monitoring at 471 nm are plotted in Figure 8. The reciprocal slope is 55.8 mV (n = 1.05), and $E^{\circ\prime}$ = −1.090 V. These figures are in excellent agreement with the observation of a reversible one-electron transfer at $(E_{1/2})_3$ = −1.105 and −1.09 V by bulk solution and thin-layer cyclic voltammetry, respectively. The combined electrochemical and spectroscopic results conclusively establish the Mo(IV)/Mo(III) couple as a reversible, monomeric one-electron redox system.

Attempts to determine $E^{\circ\prime}$ and n for the Mo(VI)/Mo(V) couple by similar procedures were frustrated by partial dimerization of the Mo(V) species, slow establishment of electrochemical equilibrium for this couple in the OTTLE cell, and partial oxidation of catechol to light-absorbing species at the longer times thus required.

Discussion

A significant result of this study is the generation of stable aqueous monomers in the Mo(III)–Mo(VI) oxidation states by electrochemical reduction of $MoO_2(cat)_2^{2-}$ at pH >9. These complexes are interconverted within a potential range of about 450 mV. Such an observation indicates that major changes in the Mo coordination environment occur at some point along the electron-transfer chain. Important contributions to these changes appear to involve (1) removal and re-formation of Mo=O bonds upon electron transfer and (2) coordination reactions at these sites when Mo=O bonds are absent. An interpretation based on these considerations is shown in Figure 9. This scheme contains three structurally distinct redox couples, Mo(VI)/Mo(V), Mo(V)/Mo(III), and Mo(IV)/Mo(III), which are interrelated by a series of redox and coordination reactions.

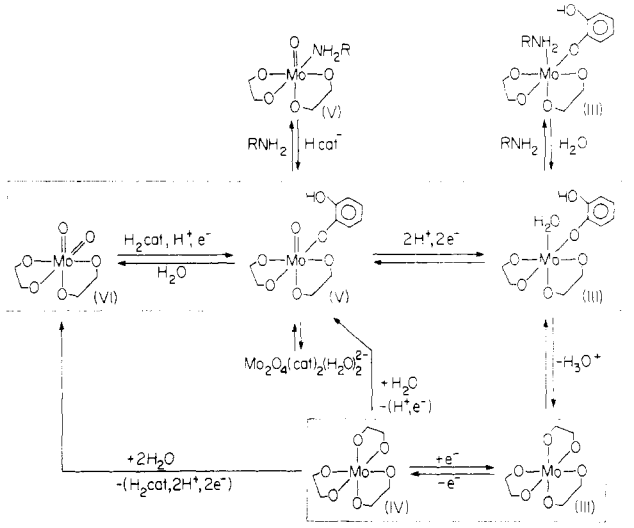

Figure 9. Electrochemical behavior of molybdenum–catechol complexes at pH >7.

Mo(VI) and Mo(V) Species. Reduction of $MoO_2(cat)_2^{2-}$ in the presence of excess catechol at pH >9 and <2 mM Mo concentration produces >80% Mo(V) monomer. This species is identified as $MoO(Hcat)(cat)_2^{2-}$ on the basis of eq 1. Its monomeric character is quantitatively established by comparative EPR and voltammetric measurements. Trachevskii and Lukachina[15] also observed EPR signals in aqueous Mo(V)–catechol solutions. These authors assigned a signal at pH 7–10 with g = 1.932 and A = 53 G to the species $MoO(H_2O)(OH)_2(cat)^-$. Their assignment appears incorrect because of the tendency of an aquo-ligated Mo(V) center to undergo dimerization. Rather, firm coordination by monodentate, monoprotonated catechol ($K_f = 1.7 \times 10^4$ M^{-1}) at the site generated by removal of one oxo group is suggested to be responsible for stabilizing the Mo(V) monomer. Coordination of catechol in this manner is facilitated by dissociation of one proton from the ligand at high pH (pK_a = 9.23).[12] Monodentate $Hcat^-$ is believed to occupy a coordination site cis to Mo=O as shown in Figure 9. This assignment is supported by the chemical and electrochemical reversibility of the Mo(VI)/Mo(V) couple (particularly in amine buffers)[9] and facile conversion of the further reduced Mo(V) compound to an apparently octahedral tris(catecholato) complex (vide infra). Thus, $MoO_2(cat)_2^{2-}$ and $MoO(Hcat)(cat)_2^{2-}$ constitute a structural pair analogous to the compounds $MoO_2(tox)_2$ and $MoOCl(tox)_2$ (tox^- = 8-mercaptoquinolinate) characterized by Yamanouchi and Enemark,[16] wherein the $Mo^{VI}O_2^{2+}$ and $Mo^{V}OCl^{2+}$ units retain a cis configuration. The (Mo(VI)/Mo(V))–catechol couple is the first example of conversion between these two forms via an electron-transfer reaction.

The appearance of a second EPR signal (g = 1.943) and intensification of the 470-nm absorption band are attributed to substitution of a monodentate amine (RNH_2 = NH_3, enH^+, or Tris) for $Hcat^-$ in the Mo(V) complex. Shifts in g value and marked intensification of the ~22 000-cm^{-1} absorption band are frequently noted effects of substitution or rearrangement of donor atoms in the MoO^{3+} coordination shell.[2,17-21] The weak EPR signal and the insensitivity of

(14) DeAngelis, T. P.; Heineman, W. R. *J. Chem. Educ.* **1976**, *53*, 594. Rohrbach, D. F.; Deutsch, E.; Heineman, W. R.; Pasternack, R. F. *Inorg. Chem.* **1977**, *16*, 2650. Rohrbach, D. F.; Heineman, W. R.; Deutsch, E. *Ibid.* **1979**, *18*, 2536.

(15) Trachevskii, V. V.; Lukachina, V. V. *Russ. J. Inorg. Chem. (Engl. Transl.)* **1976**, *21*, 62.

(16) Yamanouchi, K.; Enemark, J. H. *Inorg. Chem.* **1979**, *18*, 1626.

(17) Piovesana, O.; Furlani, C. *Inorg. Nucl. Chem. Lett.* **1967**, *3*, 535.

(18) Boorman, P. M.; Garner, C. D.; Mabbs, F. E. *J. Chem. Soc., Dalton Trans.* **1975**, 1299.

$(E_{1/2})_1$ to changes in RNH_2 concentration indicate that the extent of this substitution is slight. As in the case of $MoO(Hcat)(cat)_2^{2-}$, we believe it is most likely that RNH_2 coordinates cis to the remaining oxo group.

Molybdenum(V) monomer is not formed quantitatively at pH >9. About 10–20% of the Mo(V) appears as the dimeric di-μ-oxo species $Mo_2O_4(cat)_2(H_2O)_2^{2-}$. At pH <7 coulometric one-electron reduction of $MoO_2(cat)_2^{2-}$ produces the $Mo_2O_4^{2+}$ complex almost exclusively, but ~6% of Mo(V) monomer is observed.[1] At intermediate pH's a more equal distribution of monomers and dimers is found. These results suggest a pH- and probably catechol-dependent $2MoO^{3+} \rightleftarrows Mo_2O_4^{2+}$ equilibrium, which is shifted largely to the left at pH >9 and to the right at pH <7. Dissociation of $Mo_2O_4^{2+}$ complexes into Mo(V) monomers has been noted in many instances[22-26] in weakly acidic and alkaline solutions. However, even under the most favorable conditions only small amounts of monomer have been observed. Catechol apparently suppresses formation of oxo-bridged dimer to a greater extent than other ligands by coordinating strongly to all non-oxo sites on the MoO^{3+} center at pH >9.

Mo(IV) and Mo(III) Species. Fast-sweep-rate cyclic voltammetry (Figure 5) shows that the Mo(V) monomer formed in reaction 1 is first reduced to Mo(III) in a reversible two-electron step (reaction 6); this parallels behavior at pH <7. At slower sweep rates an intervening chemical reaction causes the reduction to split into two overlapping or closely spaced waves (Figures 4 and 5) consisting of irreversible Mo(V) → Mo(IV) reduction followed by reversible Mo(IV) ⇄ Mo(III) reduction. We propose that this reaction involves closure of the third catechol chelate ring to form an octahedral tris(catecholato) species. In agreement with this proposal we qualitatively find that the rate of the intervening reaction increases with increasing pH and decreases with increasing RNH_2 concentration (Figure 9). The Mo(III)–catechol complex so formed is oxidizable by one electron at the potential of its generation by either heterogeneous electron transfer with the electrode or homogeneous redox reaction with Mo(V). Thus, the net irreversible Mo(V) → Mo(IV) reduction consists of reaction 6 followed by reaction 9 and either reaction 10 or 11. The subsequent reversible reduction of Mo(IV) to Mo(III) is assigned to the reverse of half-reaction 10, eq 12.

$$Mo(H_2O)(Hcat)(cat)_2^{2-} \rightarrow Mo(cat)_3^{3-} + H_3O^+ \quad (9)$$

$$Mo(cat)_3^{3-} \rightleftarrows Mo(cat)_3^{2-} + e^- \quad (10)$$

$$H_3O^+ + Mo(cat)_3^{3-} + MoO(Hcat)(cat)_2^{2-} \rightarrow 2Mo(cat)_3^{2-} + 2H_2O \quad (11)$$

$$Mo(cat)_3^{2-} + e^- \rightleftarrows Mo(cat)_3^{3-} \quad (E_{1/2})_3 \quad (12)$$

Oxidation of $Mo(cat)_3^{2-}$ proceeds irreversibly to oxo–Mo(V), and –Mo(VI) species. In the OTTLE cell electrochemical reversibility of the Mo(VI)/Mo(V) couple decreases substantially, and stepwise oxidation to Mo(V) and Mo(VI) occurs.

$$H_2O + Mo(cat)_3^{2-} \rightarrow MoO(Hcat)(cat)_2^{2-} + H^+ + e^- \quad (E_{1/2})_4 \quad (13)$$

$$H_2O + MoO(Hcat)(cat)_2^{2-} \rightleftarrows MoO_2(cat)_2^{2-} + H_2cat + H^+ + e^- \quad (E_{1/2})_1 \quad (14)$$

However, at bulk mercury surfaces $(E_{1/2})_4 \gtrsim (E_{1/2})_1$, and direct irreversible two-electron oxidation to Mo(VI) is observed.

$$2H_2O + Mo(cat)_3^{2-} \rightarrow MoO_2(cat)_2^{2-} + H_2cat + 2H^+ + 2e^- \quad (15)$$

The formulation of the Mo(IV) and Mo(III) species as tris(catecholato) complexes is based upon several pieces of evidence. Binding of a third catechol molecule occurs during Mo(VI) → Mo(V) reduction; it is reasonable that its coordination should persist in the lower oxidation states. Closure of the third catechol chelate ring completes the octahedral coordination sphere around Mo with nonaquo ligands, a result which is consistent with the stability of the reduced complexes as monomers. The reversible electrochemical behavior and pH-independent half-wave potential of the Mo(IV)/Mo(III) couple suggest an electron-transfer reaction involving little structural change. In accord with our suggestion a number of tris and tetrakis complexes of transition and lanthanide metal ions (Cr^{III}, Fe^{III}, Mn^{III}, Ce^{IV})[27-32] have been prepared with catechol and catechol-like ligands. These complexes undergo reversible one-electron transfers analogous to reaction 10 or 12 in nonaqueous and alkaline aqueous media. Although we describe the species $Mo(cat)_3^{2-}$ formally as a molybdenum(IV) tris(catecholate) complex, it also could be formulated as $Mo^{III}(SQ)(cat)_2^{2-}$, where $SQ^{-\cdot}$ = *o*-semiquinone radical anion. Coordinated semiquinone has been found in a variety of Fe, Cr, Co, and Mn complexes.[29,33-37] In the closely related electron-transfer chain $Cr(dtbc)^{n-}$ ($dtbc^{2-}$ = 3,5-di-*tert*-butylcatecholate, n = 0–3),[30,32] the terminal species are best formulated as a tris(catecholato) complex of Cr(III) (n = 3) and a tris(*o*-semiquinone) complex of Cr(III) (n = 0). Electron transfer in the $Mo(cat)_3^{2-/3-}$ couple could involve some amount of ligand character, but this point must await further experimentation.

The net chemical change occurring in reactions 6, 9, and 10 or 11 is an example of electrochemically induced substitution of the type recently discussed by Saveant.[38] Other

(19) Dilworth, J. R.; McAuliffe, C. A.; Sayle, B. F. *J. Chem. Soc., Dalton Trans.* 1977, 849.
(20) Chen, G. J.-J.; McDonald, J. W.; Newton, W. E. *Inorg. Chim. Acta* **1979**, *35*, 93.
(21) Scullane, M. I.; Taylor, R. D.; Minelli, M.; Spence, J. T.; Yamanouchi, K.; Enemark, J. H.; Chasteen, N. D. *Inorg. Chem.* **1979**, *18*, 3213.
(22) Spence, J. T.; Heydanek, M. *Inorg. Chem.* **1967**, *6*, 1489.
(23) Huang, T. J.; Haight, G. P., Jr. *J. Am. Chem. Soc.* **1970**, *92*, 2336.
(24) Imamura, T.; Haight, G. P., Jr.; Belford, R. L. *Inorg. Chem.* **1976**, *15*, 1047.
(25) Haight, G. P.; Woltermann, G.; Imamura, T.; Hummel, P. *J. Less-Common Met.* **1977**, *54*, 121.
(26) Haight, G. P., Jr.; Belford, R. L.; Chapman, H. "Proceedings of the Third International Conference on the Chemistry and Uses of Molybdenum"; Barry, H. F., Mitchell, P. C. H., Eds.; Climax Molybdenum Co.: Ann Arbor, MI, 1979; pp 245–8.
(27) Raymond, K. N.; Isied, S. S.; Brown, L. D.; Fronczek, F. R.; Nibert, J. H. *J. Am. Chem. Soc.* **1976**, *98*, 1767.
(28) Cooper, S. R.; McCardle, J. V.; Raymond, K. N. *Proc. Natl. Acad. Sci. U.S.A.* **1978**, *75*, 3551.
(29) Magers, K. D.; Smith, C. G.; Sawyer, D. T. *Inorg. Chem.* **1978**, *17*, 515. *Ibid.* **1980**, *19*, 492.
(30) Sofen, S. R.; Ware, D. C.; Cooper, S. R.; Raymond, K. N. *Inorg. Chem.* **1979**, *18*, 234.
(31) Sofen, S. R.; Cooper, S. R.; Raymond, K. N. *Inorg. Chem.* **1979**, *18*, 1611.
(32) Downs, H. H.; Buchanan, R. M.; Pierpont, C. G. *Inorg. Chem.* **1979**, *18*, 1736.
(33) Wicklund, P. A.; Beckmann, L. S.; Brown, D. G. *Inorg. Chem.* **1976**, *15*, 1996.
(34) Buchanan, R. M.; Kessel, S. L.; Downs, H. H.; Pierpont, C. G.; Hendrickson, D. N. *J. Am. Chem. Soc.* **1978**, *100*, 7894.
(35) Brown, D. G.; Johnson, W. L., III *Z. Naturforsch. B: Anorg. Chem., Org. Chem.* **1979**, *34B*, 712.
(36) Buchanan, R. M.; Pierpont, C. G. *J. Am. Chem. Soc.* **1980**, *102*, 4951.
(37) Kessel, S. L.; Emberson, R. M.; Debrunner, P. G.; Hendrickson, D. N. *Inorg. Chem.* **1980**, *19*, 1170.
(38) Amatore, C.; Saveant, J. M.; Thiebault, A. *J. Electroanal. Chem. Interfacial Electrochem.* **1979**, *103*, 303. Saveant, J. M. *Acc. Chem. Res.* **1980**, *13*, 323.

examples of this behavior have been reported in transition-metal chemistry in which substitution[39] or isomerization[40] at a transition-metal center occurs with no net current flow in an electrochemical experiment. In the present case, reduction requires two electrons and reoxidation provides one; thus, a net one-electron reduction from Mo(V) to Mo(IV) is observed. This combination of redox and coordination chemistry provides a link between the redox chemistries of higher oxidation state oxomolybdenum species and lower oxidation state nonoxo species. The structural change associated with this reaction allows formation of all four oxidation states to be compressed within an energetically narrow range of 0.45 V. Thus, it is possible to observe Mo(VI)-Mo(III) catechol complexes as stable monomeric entities in aqueous solution at pH >9.

Acknowledgment. Support of this research by the National Science Foundation (Grant No. CHE 76-18703) is gratefully acknowledged. We also wish to thank Drs. J. W. McDonald, W. E. Newton, and G. D. Watt of the Charles F. Kettering Research Laboratory, Yellow Springs, OH, for their assistance in obtaining and interpreting the EPR spectra described in this work. Sue Lahr performed additional helpful experiments.

Registry No. $MoO_2(cat)_2^{2-}$, 72985-79-6; $MoO(Hcat)(cat)_2^{2-}$, 79682-15-8; $Mo(cat)_3^{2-}$, 79682-16-9; $Mo(cat)_3^{3-}$, 79682-17-0.

(39) Feldberg, S. W.; Jeftic, L. *J. Phys. Chem.* **1972**, *76*, 2439.
(40) Rieke, R. D.; Kojima, H.; Öfele, K. *J. Am. Chem. Soc.* **1976**, *98*, 6735.

Contribution from the Department of Chemistry, University of Utah, Salt Lake City, Utah 84112

Applications of Magnetic Circular Dichroism Spectroscopy: Electronic Structure of the Thiotrithiazyl Cation, $S_4N_3^+$

JACEK W. WALUK and JOSEF MICHL*

Received February 18, 1981

Magnetic circular dichroism of the $S_4N_3^+$ cation reveals the presence of four low-energy electronic transitions. Their number and properties are exactly those expected for $\pi^*-\pi^*$ excitations in a ten-π-electron system with cyclic delocalization, and they are assigned as the two L and two B bands in Platt's notation.

Introduction

The structure determination of the $S_4N_3^+$ cation[1] (**1**) showed

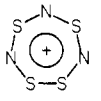

1

it to be a planar ring and prompted studies of its electronic structure.[2-4] In these, primary importance was attached to the interpretation of the electronic spectrum. We now use the technique of magnetic circular dichroism[5] to demonstrate the presence of a larger number of low-energy transitions than previously assigned or even suspected and show that the observations are in perfect agreement for $\pi^*-\pi^*$ transitions in a delocalized "aromatic" system of ten π electrons in a seven-membered ring.

Experimental Section

A sample of S_4N_3Cl, prepared according to ref 6, was provided by Professor Chivers (Calgary). The solvent used was 11 N $HClO_4$. Absorption was measured on a Cary 17 spectrophotometer and MCD on a Jasco 500C spectropolarimeter equipped with a 15-kG electromagnet.

Oscillator strengths f and the B terms were evaluated from the formulas $f = 4.319 \times 10^{-9} \int \epsilon \, d\tilde{\nu}$ and $B = -33.53^{-1} \int d\tilde{\nu} \, [\Theta]_M/\tilde{\nu}$, where $\tilde{\nu}$ is wavenumber, ϵ is the decadic molar extinction coefficient, and $[\Theta]_M$ is molar ellipticity/unit magnetic field in deg L m^{-1} mol^{-1} G^{-1}.

Calculations were performed by using the semiempirical Pariser-Parr-Pople (PPP) method as described in ref 7, including all singly excited configurations and using standard parameter values,[8] I_N = 14.1 eV, A_N = 1.8 eV, I_{S+} = 20.27 eV, A_{S+} = 10.47 eV, and β_{SN} = -1.854 eV. The value of β_{SS} was varied over a wide range with little effect on the results; the results shown in Figure 1 were obtained with β_{SS} = -1.6 eV. In the calculation of magnetic moments the procedure "2" of ref 9 was used.

Results

The absorption and MCD spectra of $S_4N_3^+$ are shown in Figure 1. The absorption spectrum is in good agreement with the previous report although the integrated oscillator strengths deviate somewhat.[2] Whereas only two bands are apparent in the absorption spectrum, a weaker one near 29 500 cm^{-1} and a stronger one near 38 000 cm^{-1}, the MCD spectrum clearly reveals the presence of four bands located near 28 500, 30 500, 37 500, and 40 000 cm^{-1} and labeled L_1, L_2, B_1, and B_2, respectively, in Figure 1. The signs of their B terms are negative for L_1 and B_1 and positive for L_2 and B_2. The results thus show that each of the seemingly simple absorption bands consists of two nearly degenerate transitions. In the case of the first absorption band, this is actually also suggested by its unsymmetrical shape. The magnitudes of the B terms suggest that they are dominated by the mutual mixing of the L_1 and L_2 states and of the B_1 and B_2 states by the magnetic field, although the inequality of the magnitudes of $B(L_1)$ and $B(L_2)$ indicates that the situation is not quite so simple.

Discussion

The planar cyclic structure of $S_4N_3^+$, which guarantees considerable π overlaps, and a simple electron count invite the thought that this cation must be a rare representative of a delocalized ten-π-electron seven-membered ring system, iso-

(1) J. Weiss, *Z. Anorg. Allg. Chem.*, **333**, 314 (1964); A. W. Cordes, R. F. Kruh, and E. K. Gordon, *Inorg. Chem.*, **4**, 681 (1965).
(2) D. A. Johnson, G. D. Blyholder, and A. W. Cordes, *Inorg. Chem.*, **4**, 1790 (1965).
(3) P. Friedman, *Inorg. Chem.*, **8**, 692 (1969).
(4) R. D. Harcourt, *J. Inorg. Nucl. Chem.*, **39**, 237 (1977).
(5) P. J. Stephens, *Annu. Rev. Phys. Chem.*, **25**, 201 (1974).
(6) N. Logan and W. L. Jolly, *Inorg. Chem.*, **4**, 1508 (1965).
(7) A. Castellan and J. Michl, *J. Am. Chem. Soc.*, **100**, 6824 (1978).
(8) R. Zahradnik, A. J. Banister, and H. G. Clarke, *Collect. Czech. Chem. Commun.*, **38**, 998 (1973).
(9) N. H. Jørgensen, P. B. Pedersen, E. W. Thulstrup, and J. Michl, *Int. J. Quantum Chem.*, **12S**, 419 (1978).

0020-1669/82/1321-0556$01.25/0